ChemPubSoc Europe

DOI: 10.1002/cptc.201900175

CHEMPHOTOCHEM Articles

Intra- and Intermolecular Fluorescence Quenching of Alkylthio-Substituted Phthalimides by Photoinduced Electron Transfer: Distance, Position and Conformational Dependence

Murat Atar,[a] Banu Öngel,[a] Henrik Riedasch,[a] Tim Lippold,[a] Jörg Neudörfl,[a] Diego Sampedro,[b] and Axel G. Griesbeck*[a]

The photophysical properties of fluorescent phthalimides with thioether groups directly connected to the chromophore or separated by alkyl spacers, respectively, were studied. Intermolecular fluorescence quenching by electron transfer from dimethylsulfide to the 4,5-dimethoxy phthalimide (DMPht) model compound **6** is dynamic and fast. The fluorescence properties of **6** and the remote C_5-spaced thioether derivative **5** are nearly identical. In compounds **1**–**4** with shorter spacer lengths, fluorescence quenching is strong for C_2 and C_3-spaced **2** and **3** and less pronounced for C_1- and C_4-spaced compounds **1** and **4**, mapping the conformational landscape of these molecules. The *o*-,*m*-,*p*-substituted N-(thiomethyl)benzyl DMPht **7** are almost non-fluorescent which correlates very well with the intermolecular thioanisole fluorescence quenching of **6**. In contrast, the 3- and 4-thiomethyl phthalimides **8** and **9** show divergent fluorescence that is also rationalized by DFT calculation results. The fluorescence properties can be switched by oxidation of the thioethers to sulfoxides with H_2O_2 or $^1O_2$ (*off*→*on* for **1**,**4**,**7** and *on*→*off* for **9**). Further functionalized molecules that were based on the model compounds are the sulfur-containing amino acid methionine derivative **10**, dipeptides **11a**,**b**, and S-alkylated cysteine derivatives **12** to **14a**–**d** with strong side-chain-dependent fluorescence.

1. Introduction

The fluorescence behavior of chromophores with tunable nπ*/ππ*-excitation modes is fascinating because a slight change in substitution pattern or solvent properties strongly influences the initial photophysical processes, absorption wavelengths and absorbance, intersystem crossing rates and efficiencies, radiationless decay and emission from the lowest singlet and triplet states.[1] If these excited states are in a suitable energetical order and distance, singlet-triplet intersystem crossing can be extremely fast due to complied El-Sayed rules,[2,3] e.g. in the perfect example benzophenone[4] and also in the unsubstituted and N-arylated phthalimides.[5] Some of these compounds show fluorescence quantum yields <0.001 and ISC quantum yields $>95\%$. The parent phthalimide was initially described by Coyle as a three near-lying excited state system (S_1 ππ*, S_2 nπ*, T_2 ππ*) with a lower lying T_1 nπ*.[6,7] A recent study on the femto- and picosecond time-resolved spectroscopy of N-methylphthalimide revealed the existence of two lowest singlet ππ* states, the higher state non-emissive with ε about 2000, the lowest singlet not detectable by absorption spectroscopy but by fluorescence ($\Phi_F \approx 0.01$) leading to large apparent Stokes shifts $>10.000\ cm^{-1}$.[8] We have in the last two decades used the unsubstituted phthalimide as an excellent one-electron acceptor in its excited triplet states T_2/T_1, e.g. for photodecarboxylation reactions in intra- and intermolecular processes.[9–11] In order to switch from the parent non-fluorescent phthalimide chromophore to a stronger fluorophore, the introduction of one or two donor groups at the positions C3 and/or C4 is advisable. Alkoxy and amino (or amido) groups directly coupled to the chromophore are the optimal groups for fluorescence increase and absorption redshift.[12–14] An especially successful approach was the 4,5-dialkoxyphthalimide that shows strong fluorescence with quantum yields near to 100%.[15] Strongly fluorescent phthalimides that also constitute very strong reductants in the excited singlet states have been developed as excellent sensors for anions such as fluoride,[16,17] or cyanide.[18] Recently, we have developed phthalimide probes for singlet oxygen and hydrogen peroxide that operate by fluorescence ON effects and were based on 4,5-dialkoxyphthalimides with internal fluorescence quenching groups.[19] This concept is based on the known

[a] Dr. M. Atar, B. Öngel, H. Riedasch, T. Lippold, Dr. J. Neudörfl, Prof. Dr. A. G. Griesbeck
Department of Chemistry
University of Cologne
Greinstr. 4, D-50939 Köln (Germany)
Fax: (+0049) 221 4701166
E-mail: griesbeck@uni-koeln.de
Homepage: http://www.oc.uni-koeln.de/griesbeck/

[b] Prof. Dr. D. Sampedro
Departamento de Química
Universidad de La Rioja
Madre de Dios 53, E-26006 Logroño (Spain)

Supporting information for this article is available on the WWW under https://doi.org/10.1002/cptc.201900175

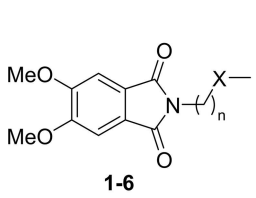

	X=	n=
1	S	1
2	S	2
3	S	3
4	S	4
5	S	5
6	CH_2	2

Figure 1. 4,5-Dimethoxyphthalimide standard **6** and thioethers **1**–**5**.

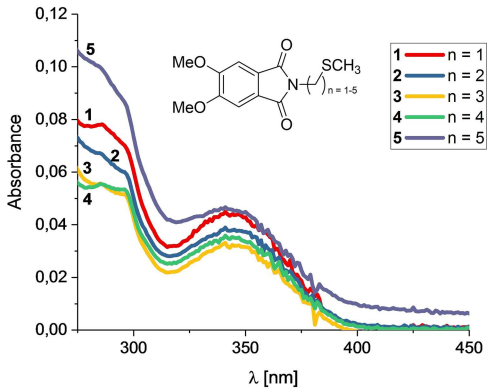

Figure 2. UV/Vis absorption spectra of thioethers **1**–**5** in CH_3CN (2×10^{-5} M).

fluorescence quenching/sensor properties of thiols[20,21] and thioethers with respect to phthalimide chromophores.[15] In this paper, we describe an extensive study of the photophysical properties of thioalkylated and thioarylated phthalimides and the corresponding structural interpretations of their fluorescence properties.

2. Results and Discussion

2.1. Intramolecular Fluorescence Quenching: Alkyl Thioethers

The fluorescence properties of a homologous series of 4,5-dimethoxy phthalimides **1**–**5** with thiomethyl-terminated alkyl chains at the imide nitrogen (Figure 1) were investigated by static and time-resolved methods and compared with the strongly fluorescent N-butyl compound **6** as the reference standard. All phthalimides for this study were synthesized either by thermal condensation of phthalic anhydride with the corresponding amines or by substitution reactions of the N-bromoalkylphthalimides with sodium methylthiolate (see the Supporting Information), respectively, and purified by recrystallization. In the absorption spectra, the long-wavelength maxima and the corresponding extinction coefficients are nearly identical (342 ± 2 nm) for all compounds (Figure 2, Table 1).

In contrast to these highly similar ground-state properties, the excited state behavior of **1**–**5** strongly depends on the position of the thioether group. The fluorescence of compound **1** with the shortest linker between phthalimide and the thioether group showed a roughly halved fluorescence intensity compared with the undistorted **5** or the unfunctionalized **6** (Figure 3). The C_2- and C_3-spaced **2**,**3** showed fluorescence

Table 1. Fluorescence properties of thiomethyl-functionalized 4,5-dimethoxy phthalimides **1**–**5** and the *n*-butyl derivative **6**.

	λ_{abs}[a] [nm]	log ε	λ_{em}[b] [nm]	Stokes[c] [cm^{-1}]	Φ_F[d]	τ_F (%) [ns][e]
1	341	3.27	439	6546	0.32	29.3 (66); 1.2 (34)
2	340	3.26	443	6838	0.06	14.5 (4); 3.1 (96)
3	342	3.24	441	6564	0.04	30.6 (71); 0.7 (29)
3	345[f]	3.2[f]	447[f]	6614	0.04[f]	n.d.
4	343	3.26	444	6631	0.31	19.0 (91); 6.9 (9)
5	342	3.34	444	6717	0.55	31.3 (100)
6	344	3.28	444	6547	0.61	31.9 (100)

[a] In acetonitrile, r.t., 2×10^{-5} M solutions; [b] In acetonitrile, r.t., 10^{-5} M solutions; [c] $(E_{abs}[cm^{-1}])-(E_{em}[cm^{-1}])$; [d] Determined vs. quinine sulfate; [e] By TCSPC fluorescence spectroscopy; [f] In CH_2Cl_2, from Ref. [15]; n.d. = not determined.

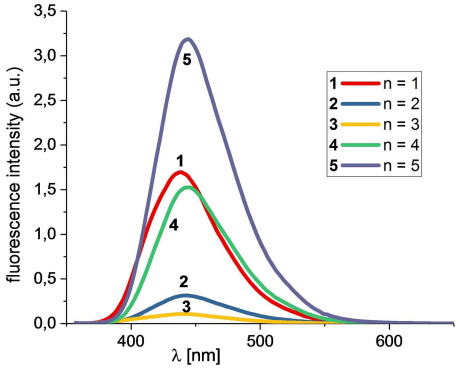

Figure 3. Fluorescence spectra of thioethers **1**–**5** in CH_3CN (10^{-5} M).

reduction to $<10\%$ intensity, whereas the C_4-spaced **4** showed similar behavior as compound **1**. Thus, electron transfer quenching, the key process that apparently reduces the fluorescence of these compounds, goes through a maximum at medium donor-acceptor (Do-Acc) distances and gets marginalized at short and long distances.

All fluorescence signals of the covalently linked phthalimide-thioethers **1**–**5** could be easily time-resolved by time correlated single-photon counting (TCSPC). The respective fluorescence decays were fitted by single or biexponential decays convoluted with the instrumental response function (IRF). Only compound **5** (and of course also the standard molecule **6**) could be cleanly fitted with a monoexponential function leading to a fluorescence lifetime of 31.3 ns (Table 1).

This value for this donor-acceptor molecule **5** is nearly identical to the lifetime of the reference molecule **6** with a CH_2 group instead of the thioether sulfur atom (31.9 ns), i.e. a non-quenching functionality. In addition, the fluorescence quantum yields of **5** and **6** are also nearly identical with values of 0.55 and 0.61. From the biexponential fitting of the decay traces of compounds **1**–**3**, one short lifetime (1–3 ns) resulted that dominated **2** and was a minor component of **1** and **3**. The longer lifetime component (15–30 ns) nearly disappears in **2** but dominates fluorescence in **1** and **3**. Compound **4** has two fluorescent components with comparable lifetimes (19 and 7 ns) with the longer-lived component dominating (91:9). Because of the obviously very weak ground-state interactions

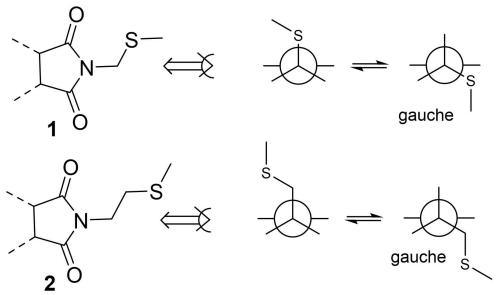

Figure 4. The conformational landscape for substrates **1** and **2** with orthogonal and gauche thioalkyl substituents.

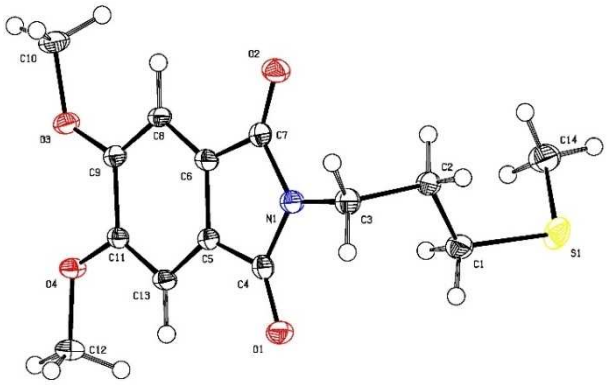

Figure 5. Structure of compound **3** in the crystal (ORTEP plot, thermal ellipsoids set at 50% probability).

(no differences in the absorption spectra), these results have to be interpreted as a visualization of the slow (on the nanosecond timescale of fluorescence) equilibrium of the alkylthio side chain, i.e. mapping the *conformational landscape* of these compounds (Figure 4). In compound **1**, only two equilibrating conformers are possible with the orthogonal or gauche orientation of the methylthio group with respect to the chromophore π-system. The fluorescence decay of **1** consists of two components, one short-lived and one long-lived (the latter similar to the non-quenchable **6**) in nearly identical composition whereas the homologous **2** shows nearly exclusively the short-lived component and thus intramolecular ET-quenching geometries dominate here. The longer the hydrocarbon spacer chain, the less prominent becomes the short-lived component and the >20 ns component prevails.

The C_3-spaced compound **3** could also be characterized by crystal structure analysis and shows a preferred N(CC)C-synclinal (gauche) conformation in the solid state (Figure 5). This geometry appears the most favorable arrangement for intramolecular electron transfer and fluorescence is nearly completely quenched for this compound ($\Phi_F = 0.04$ in acetonitrile and methylene chloride).

Thus, it appears that gauche conformers, in general, tend to rapid fluorescence quenching by electron transfer. In the C_4-spaced compound **4**, two fluorescent species appear with comparable contributions and lifetimes that accounts for gauche geometries (like in compound **3**) with the thiomethyl group in more remote positions. Eventually, the electron donating thioether is completely separated from the acceptor group on the conformational landscape in the C_5-spaced compound **5** and restores the long-lived fluorescent species with monoexponential decay. This rationalization of the fluorescence decay data is valid only for the nanosecond time regime that we are dealing with for the 4,5-dimethoxy phthalimides **1**–**5**.

In the case of the non-fluorescent phthalimides with similar or even more remote thioether side-chains, the corresponding triplets have microsecond lifetimes and are also efficiently deactivated by electron transfer. Photoinduced electron transfer and subsequent proton transfer leads to triplet biradicals that combine to medium- and large-ring cycles, e.g. from the phthalimides **3-H** and **5-H**, respectively (Figure 6).[22–24] This happens neither with the fluorescent 4,5-dimethoxy phthalimide **3** nor with the fluorescent **5**, and thus, electron transfer quenching, e.g. from **3**, is followed by rapid back electron transfer.

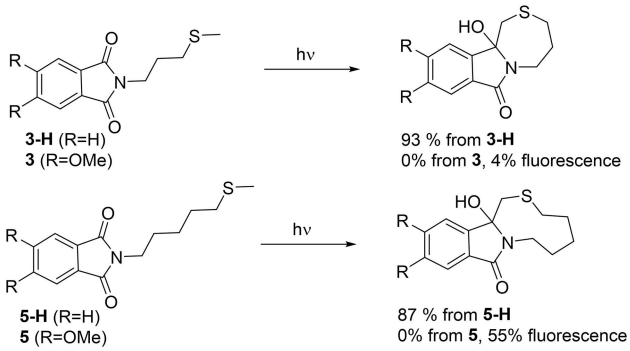

Figure 6. Photochemistry of the fluorescent/non-fluorescent 4,5-dimethoxy phthalimides **3**, **5** versus the unsubstituted analogues.

2.2. Intermolecular Fluorescence Quenching

In order to better understand the intramolecular effects, the absolute rates of electron transfer from methyl alkyl sulfides to DMPht are important values. The fluorescence quenching of the model compound 3,4-dimethoxy N-methyl phthalimide (DMMP) by dimethyl sulfide was recently investigated and dynamic quenching with a Stern-Volmer constant K_{SV} of 59 M^{-1} was determined in methylene chloride.[15] In order to correlate this with the compounds described in this publication, the N-butyl derivative **6** was investigated and also fluorescence lifetimes were determined for **6** and the N-methyl derivative in acetonitrile. In acetonitrile, the undisturbed fluorescence of phthalimide **6** decays monoexponential with $\tau_F = 32$ ns and is quenched by external dimethylsulfide (Figure 7). No additional absorption or emission signals appear even at high quencher concentrations and the fluorescence intensity decrease parallels lifetime decrease (Figure 8), though with a slight diversion in the high concentration region.

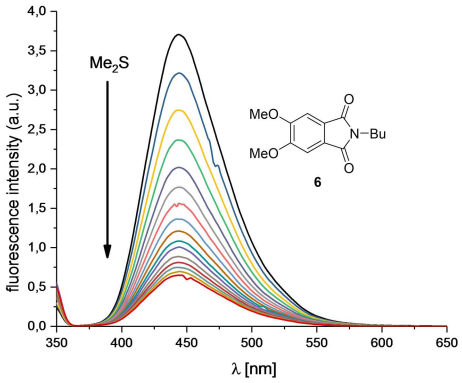

Figure 7. Fluorescence spectra of **6** in CH_3CN with increasing amounts of Me_2S.

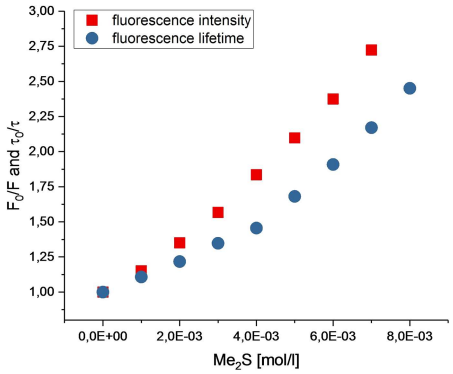

Figure 8. Stern-Volmer concentration (Me_2S) plots versus fluorescence intensity and fluorescence lifetimes for **6** in CH_3CN.

From the intensity analysis, we determined a Stern-Volmer constant of 4.3 ($=1.3\times10^8\ M^{-1}s^{-1}$ for dynamic quenching), more than 10 times lower than the literature value for DNMP in CH_2Cl_2. This is good accord with the lower positive Coulombic energy term E_C in the more polar acetonitrile ($E_c=0.06$ eV)[25] and the supposable small but detectable steric shielding effect of the N-butyl substituent.

In order to further investigate the nature of the quenching event and the consistency of the quenching constants, we investigated other thioethers, phosphanes, and amines as fluorescence quenchers (Table 2) and compared the effects on fluorescence intensities and lifetimes. No additional lifetimes were found throughout all analyses, indicating a single quenching mechanism. Steric effects can be expected for the $(tBu)_2S$ vs. Me_2S and actually, a tenfold reduction in quenching rate was observed which also corresponds to the lower free energy of electron transfer as calculated from the Rehm-Weller approximation.[26] Thioanisole is a much stronger quencher which apparently does not correlate with the electrochemical properties (oxidation potentials of the thioethers). Triphenylphosphane and the corresponding tributyl compounds are even better reductants and fast dynamic quenching is registered with these compounds. Eventually, triethylamine and Hünig-base ($N(iPr)_2Et$) are expected to undergo electron transfer to the excited singlet phthalimide **6** with roughly 1 eV exergonicity and thus, near diffusion-controlled fluorescence quenching ($7–8\times10^9\ M^{-1}s^{-1}$) is detected.

The fluorescence intensity / concentration plots are linear over a large concentration area; the fluorescence lifetime / concentration correlation becomes non-linear for higher concentrations of dimethyl sulfide (which is not the case for most other quenchers) indicating some static quenching fraction at higher concentration. The Stern-Volmer constants have very good correlation and were calculated from lower to moderate quencher concentration areas.

2.3. Intramolecular Fluorescence Quenching: Sulfoxides

The oxidation potentials of dimethylsulfide and the corresponding sulfoxide DMSO are only 250 mV separated[28] and thus, electron transfer should still be energetically feasible and detectable at least in the intramolecular cases studied herein. The sulfide oxidation of all thioethers **1**–**5** was selectively performed by photooxygenation in acetonitrile with rose bengal (RB) as the singlet oxygen sensitizer. These reactions are known to stop at the sulfoxide level and no further oxidation to the corresponding sulfones does occur. We could prove this by NMR analyses for all substrates **1**–**5** which were selectively oxidized to the sulfoxides $\mathbf{1}^{S=O}$ to $\mathbf{5}^{S=O}$. The comparison between fluorescence behavior of the sulfide vs. the corresponding sulfoxides (Table 3) revealed that the relative

Table 2. Fluorescence quenching properties of the 4,5-dimethoxy-phthalimide **6** by S,P,N quenchers.

Q[a] [M]	K_{SV} [b] [M^{-1}]	k_q [c] [$M^{-1}s^{-1}$]	$E^0(Q^+/Q)$ [d] [V] vs. SCE	ΔG^0_{PET} [e] [eV]
$(tBu)_2S$	0.4	1.4×10^7	1.59	−0.19
Me_2S	4.3	1.3×10^8	1.37	−0.41
PhSMe	113.5	3.5×10^9	1.44	−0.34
PPh_3	109.8	3.4×10^9	1.06	−0.72
$P(nBu)_3$	64.1	2.0×10^9	1.16	−0.62
NEt_3	236.5	7.4×10^9	0.83	−0.95
$N(iPr)_2Et$	262.4	8.1×10^9	0.68	−1.10

[a] in CH_3CN, r.t., 10^{-5} M solutions **6**; [b] $Ksv=F_0/F[Q]$; [c] $k_q=Ksv/32$ ns; [d] s. SCE in CH_3CN (Ref. [27]); [e] from $\Delta G=F[E^0(Q^+/Q)–E^0(\mathbf{6}/\mathbf{6}^-)]-E_{00}(\mathbf{6})-E_c$ with $E^0(\mathbf{6}/\mathbf{6}^-)=-1.59$ V (vs. SCE, Ref. [19]), $E_{00}(\mathbf{6})=3.31$ eV (Ref. [15]) and $E_c=0.06$ eV (Ref. [25]).

Table 3. Fluorescence properties of the sulfur-oxidized thiomethyl-functionalized 4,5-dimethoxyphthalimides **1**–**5**.[a]

	$\lambda_{em}\rightarrow\lambda_{em}^{S=O}$[b] [nm]	$\Phi_F\rightarrow\Phi_F^{S=O}$[c]	τ_F [ns][d] sulfoxide
$\mathbf{1}\rightarrow\mathbf{1}^{S=O}$	439→451	0.32→0.32	22.0
$\mathbf{2}\rightarrow\mathbf{2}^{S=O}$	443→448	0.06→0.26	30.7
$\mathbf{3}\rightarrow\mathbf{3}^{S=O}$	441→447	0.04→0.25	30.2
$\mathbf{4}\rightarrow\mathbf{4}^{S=O}$	444→450	0.31→0.53	31.6
$\mathbf{5}\rightarrow\mathbf{5}^{S=O}$	444→450	0.55→0.63	32.6
6	444	0.61	31.8

[a] Oxidation with $^1O_2$ in CH_3CN (RB, hν, $^3O_2$), r.t., 10^{-3} M solutions of **1**–**5**; [b] change in emission maxima with complete oxidation; [c] change in fluorescence quantum yields with complete oxidation; [d] by TCSPC fluorescence spectroscopy, all monoexponential decays.

fluorescence intensity decrease that was measured for the "short-spacer" compound **1** is completely preserved for the corresponding sulfoxide, whereas as other compounds showed an increase in fluorescence intensities. There is only one fluorescent species for all sulfoxide-containing compounds and one can, therefore, speculate, e.g. for the shortest linker phthalimide $\mathbf{1}^{S=O}$, that only the perpendicular conformer is populated that we also identified to be the most prominent electron transfer component for **1** (Figure 9).

The time course of the singlet oxygen reaction of thioether **3** is shown in Figure 10. During irradiation of a 10^{-5} M solution of rose bengal (RB) in acetonitrile, there is a constant increase in global fluorescence due to the formation of the oxidized form $\mathbf{3}^{S=O}$, accompanied by a slow degradation of the dye (emission decrease at 580 nm). The fluorescence quantum yield increases from 4% to 25% with a slight shift in emission maximum. Thioalkylated compounds such as **2** and **3**, therefore, appear useful as probes for singlet oxygen, but only if they exhibit strong internal fluorescence quenching in the non-oxidized states.[19]

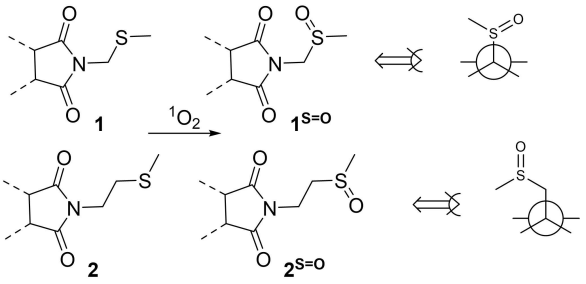

Figure 9. Formation and preferred conformers of compounds $\mathbf{1}^{S=O}$ and $\mathbf{2}^{S=O}$.

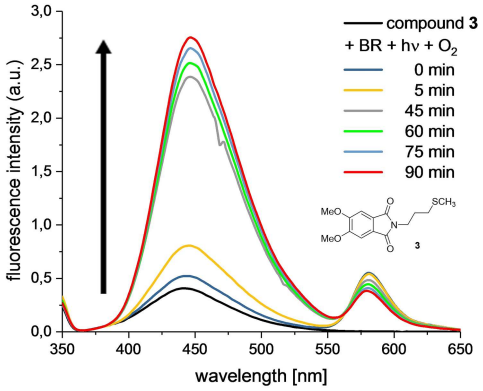

Figure 10. Fluorescence spectra of **3** in CH_3CN under $^1O_2$ sensitization.

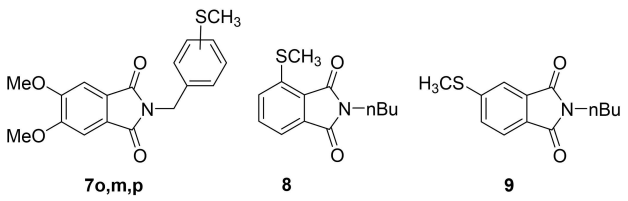

Figure 11. Three regioisomeric N-thiomethyl-benzylated phthalimides **7o**,**m**, **p** and the directly chromophore-modified phthalimides **8** and **9**.

2.4. Intramolecular Fluorescence Quenching: More Complex Substrates and Substrates from Amino Acids

The strong intermolecular fluorescence quenching of **6** by thioanisole (Table 2) indicates that aromatic thioethers constitute much more efficient electron donors than aliphatic thioethers despite similar oxidation potentials. This effect should also show up in intramolecular versions and thus, we prepared and studied the excited behavior of the regioisomeric thiomethylbenzyl phthalimides **7o**–**7p**. Actually, all three regioisomeric compounds showed very similar behavior: low fluorescence quantum yields and Stokes shifts around 6600 cm^{-1}. The only remarkable difference is that the longer-lived transient (τ_F between 22 and 25 ns) dominates the emission from meta and para compounds whereas a short-lived component ($\tau_F = 1.5$ ns) dominates for the ortho derivative **7o** (Table 4). Similar effects as for **7o** were observed for the 3-thiomethyl phthalimide **8** that showed nearly no fluorescence. This effect appears, however, not to be a consequence of PET effects because also the corresponding sulfoxide $\mathbf{8}^{S=O}$ is not emissive. In contrast to **8**, the 4-thiomethyl compound **9** shows strong fluorescence that completely disappeared upon oxidation to the sulfone $\mathbf{9}^{SO2}$ (the intermediary sulfoxide could not be isolated).

Table 4. Fluorescence properties of the isomeric N-thiomethylbenzylated 4,5-dimethoxy phthalimides **7o**, **m**, **p** and the DMPI-substituted **8** and **9**.

	λ_{abs} [a] [nm]	log ε	λ_{em} [b] [nm]	Stokes [cm^{-1}][c]	Φ_F [d]	τ_F (%) [ns][e]
7o	342	3.30	444	6717	0.07	27.5 (32); 1.5 (68)
7m	343	3.29	444	6632	0.08	21.9 (93); 0.5 (7)
7p	345	3.26	443	6412	0.09	24.7 (95); 0.4 (5)
8	367	3.60	451	5075	0.04	1.3 (100)
9	346	3.58	455	6923	***0.56***	***15.1 (100)***
$\mathbf{9}^{SO2}$	350	3.43	–	–	–	–

[a] In acetonitrile, r.t., 2×10^{-5} M solutions; [b] in acetonitrile, r.t., 10^{-5} M solutions; [c] (E_{abs}[cm^{-1}])−(E_{em}[cm^{-1}]); [d] determined vs. quinine sulfate; [e] by TCSPC fluorescence spectroscopy.

The differences in fluorescence properties for the regioisomeric compounds **8** and **9** is remarkable and indicates an active non-radiative deactivation channel for the singlet excited state of **8** that is not operating for **9**-in accord with the theoretical investigation (*vide infra*). In continuation of our work on singlet oxygen probes based on methionine derivatives,[19] we also looked at derivatives of **3** which actually constitutes the decarboxylated 4,5-dimethoxyphthaloyl methionine (Figure 12). In order to avoid photodecarboxylation, the methyl esters of methionine (**10**) and the dipeptides Met-Gly and Met-Pro **11a** and **11b**, respectively, were investigated. As additional compounds with shorter linker chains, we also studied the S-methyl cysteine derivative **12** and the S-unprotected **13**.

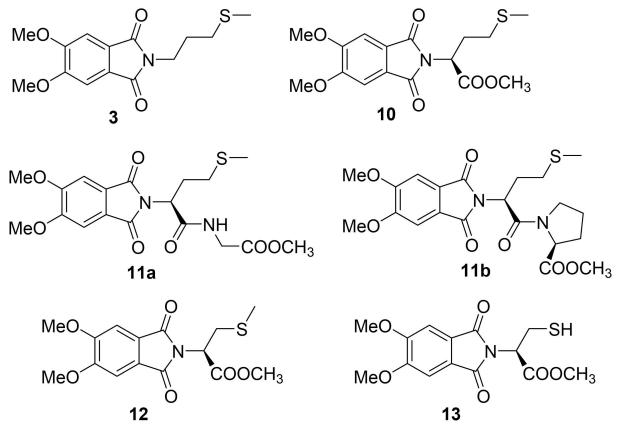

Figure 12. Three methionine-derived (**10**, **11a**,**b**) and two cysteine-derived (**12**, **13**) 4,5-dimethoxyphthalimides in comparison with model compound **3**.

Table 5. Fluorescence properties of the 4,5-dimethoxy phthalimide methionine (**10**,**11**) and cysteine derivatives **12**, **13** (**3** for comparison).

	λ_{abs} [a] [nm]	log ε	λ_{em} [b] [nm]	Stokes [cm^{-1}][c]	Φ_F [d]	τ_F (%) [ns][e]
3	342	3.24	441	6564	0.04	30.6 (71); 0.7 (29)
10	344	3.39	440	6342	0.04	28.7 (87); 0.5 (13)
11a	345	3.26	450	6763	0.08	33.7 (70); 0.7 (30)
11b	343	3.39	445	6683	0.03	32.5 (70); 0.66 (30)
12	347	3.39	445	6347	0.17	25.2 (62); 0.7 (38)
13	347	3.45	443	6245	0.64	27.4 (100)

[a] In acetonitrile, r.t., 2×10^{-5} M solutions; [b] in acetonitrile, r.t., 10^{-5} M solutions; [c] (E_{abs}[cm^{-1}])−(E_{em}[cm^{-1}]); [d] determined vs. quinine sulfate; [e] by TCSPC fluorescence spectroscopy.

The data in Table 5 shows that, in accord with the data for **3**, all C_3-spaced compounds showed low fluorescence quantum yields with biexponential decay, whereas the C_2-spaced cysteine derivative **12** has a 0.17 quantum yield of fluorescence with a dominating contribution from a 25 ns component. Surprisingly, the 4,5-dimethoxyphthaloyl cysteine (methyl ester **13**) decays monoexponential with a 27.4 ns component and 0.64 fluorescence quantum yield and thus is nearly identical to the undisturbed model compound **6**. In order to find a rationale for this effect, we investigated the C2-spaced thioethers **14a**–**14d** (Figure 13) and compared the results with the methylthio compound **2** (Table 6). From compound **14a**, a crystal structure analysis was obtained (Figure 14), again

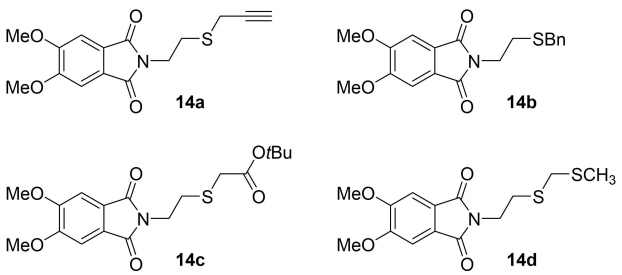

Figure 13. Four N-thioethyl-spaced phthalimides **14a**–**d**.

Table 6. Fluorescence properties of the N-thioethyl-4,5-dimethoxy-phthalimide **15a**–**15d** (**2** for comparison).

	λ_{abs} [a] [nm]	log ε	λ_{em} [b] [nm]	Stokes [cm^{-1}][c]	Φ_F [d]	τ_F (%) [ns][e]
2	340	3.26	443	6838	0.06	14.5 (4); 3.1 (96)
14a	339	3.25	442	6874	0.47	23.7
14b	343	3.36	443	6581	0.12	14.5 (4); 3.1 (96)
14c	342	3.21	450	7017	0.39	16.9
14d	345	3.33	444	6463	0.12	27.6 (49); 3.2 (51)

[a] In acetonitrile, r.t., 2×10^{-5} M solutions; [b] in acetonitrile, r.t., 10^{-5} M solutions; [c] (E_{abs}[cm^{-1}])−(E_{em}[cm^{-1}]); [d] determined vs. quinine sulfate; [e] by TCSPC fluorescence spectroscopy.

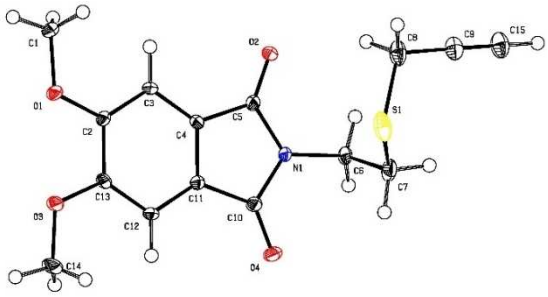

Figure 14. Structure of the highly fluorescent **14a** in the crystal (ORTEP plot, thermal ellipsoids 50% probability).

(compare with compound **3** in Figure 5) revealing a preferred gauche orientation at C1-C2.

In general, the thiomethyl compound **2** shows the strongest quenching contribution and thus the lowest fluorescence quantum yield. In contrast to naïve expectations, electron donor, as well as acceptor substitution at the thioether sulfur, did intensify the fluorescence channel. Weaker contributions were detected from the benzyl group in **14b** and the methylthiomethyl (MTM) group in **14d** (doubling of Φ_F). The ester and especially the propargyl substituted compounds **14c** and **14a**, respectively, are strongly emissive and decay monoexponential with 17 and 24 ns, respectively. This is probably due to electronic deactivation of the thioether group (similar for compound **13**). The series of cysteine analogs **14a**–**d** thus reveals that slight changes in the side-chain of fluorogenic chromophores can lead to drastic changes in the deactivation channels.

2.5. Emission of Chromophore-Modified 8 and 9: Theoretical Calculations

As shown above, the absorption properties of the regioisomeric thiomethyl-derivatives of the N-butyl phthalimide **8** and **9** are very similar. In contrast, the emission properties are clearly different (see Table 4). In order to clarify this issue, we performed a series of theoretical calculations on the optical properties of **8** and **9** in the framework of the density functional theory (DFT). First, we explored the absorption spectra of **8** and **9** using two commonly used functionals (CAM-B3LYP and

Table 7. Optical properties of phthalimides **8** and **9** in acetonitrile.

	λ_{abs} [nm] CAM-B3LYP	λ_{em} [nm] CAM-B3LYP	*f* CAM-B3LYP	λ_{abs} [nm] B3LYP	λ_{em} [nm] B3LYP	*f* B3LYP
8	330	390	0.11	395	464	0.08
9	320	398	0.15	383	458	0.14

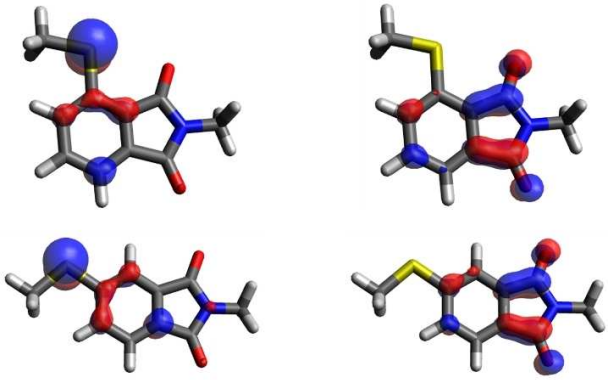

Figure 15. HOMO (left) and LUMO (right) orbitals for phthalimides **8** (top) and **9** (bottom).

B3LYP) together with the standard basis set 6-31 + G(d,p) and including the solvent effect (acetonitrile) through the Polarizable Continuum Model (PCM). The results are summarized in Table 7.

In agreement with the experimental results, the computed absorption properties of **8** and **9** are similar, with a n->π* transition responsible for the band at longer wavelengths. The orbitals involved in these transitions are also equivalent in both compounds (Figure 15).

Also, both compounds relax on the excited state potential energy surface to populate an equivalent minimum in S_1 (SI, Figure S2). From there, emission could take place as experimentally found. The difference between **8** and **9** appears with an alternative deactivation channel that may be active for **8** but not for **9**. In the case of **8**, the proximity between the S and O atoms opens up the possibility of a geometrical deformation that allows those atoms to interact. This was explored by means of a relaxed scan in which the S–O distance was modified (Figure 16). In this case, the B3LYP functional was used as better results for the excited state properties were found (Table 7).

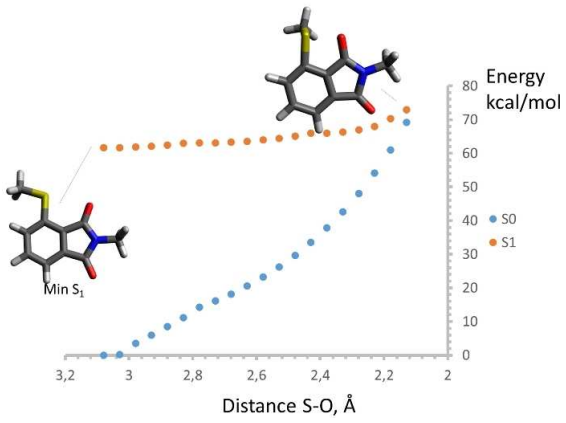

Figure 16. Relaxed scan along the singlet excited state potential energy surface for **8**.

After the population of the S_1 minimum, two competitive pathways arise for **8**. On one hand, radiative deactivation implies the emission as detected experimentally. On the other hand, a relatively small geometrical deformation (SCH_3 out-of-plane rotation and S–O distance decrease) allows reaching a region of degeneracy between S_1 and S_0 at a low energetic cost. Thus, the ground state could be easily recovered, causing a reduction in the fluorescence quantum yield and the excited state lifetime, in agreement with the experimental results. Clearly, this non-radiative deactivation channel cannot operate in the case of **9**, and the emission remains the major deactivation pathway.

3. Summary and Conclusions

The absorption and fluorescence properties of a series of 4,5-dimethoxyphthalimides (DMPht) with thioether groups in the side-chain of this fluorogenic chromophore was investigated. Additionally, the two chromophore-modified regioisomeric phthalimides **8**, **9** with methylthio groups at C3 and C4 were studied. The absorption properties of all DMPht derivatives differed only marginally from the standard compound **6** with no quencher functionality in its side-chain. Thus, there is no ground-state interaction between the imide electron acceptor and the thioether electron donor. This changes completely for the excited singlet states and the fluorescence quantum yields range from 0.64 (for **13**) to 0.03 (for **11b**). Chain dynamics and electronic effects direct the fluorescence quenching process that is most likely electron transfer driven as apparent from the comparison with the results from intermolecular quenching kinetics with aliphatic and aromatic thioethers and the standard substrate **6**.

The distance dependence of fluorescence for compounds **1**–**5** (with methylene spacer lengths 1 to 5) reflects the well-known and extensively studied "n = 3 rule" that was initially reported by Hirayama for the highly efficient formation of intramolecular exciplexes with trimethylene tethers.[29,30] This rule is valuable for the prediction of the most reactive substrate for intramolecular photochemical processes[31] or for the formation of intramolecular exciplexes.[32,33] The structural rationale of this empirical rule is the alkyl chain dynamics and the two X-ray structures analyses that we have determined for **3** (n = 3) and **14a** (n = 2) show, that the alkyl chain conformation has a gauche twist after the second tether carbon which favors donor-acceptor interaction especially in the n = 3 compound. Supposedly, a similar behavior exist in solution-phase that makes charge transfer processes efficient. This effect is independent on substituents in the linker chain (see Table 8, right column). All representatives with n = 3 show low fluorescence quantum yields between 3% and 8%. The

Table 8. Fluorescence properties of $n=2$ and $n=3$ phthalimides.

$n=2$	Φ_F	τ_F (%) [ns]	$n=3$	Φ_F	τ_F (%) [ns]
2	0.06	14.5 (4); 3.1 (96)	**3**	0.04	30.6 (71); 0.7 (29)
12	0.17	25.2 (62); 0.7 (38)	**10**	0.04	28.7 (87); 0.5 (13)
14a	0.47	23.7 (100)	**11a**	0.08	33.7 (70); 0.7 (30)
14b	0.12	14.5 (4); 3.1 (96)	**11b**	0.03	32.5 (70); 0.66 (30)

dominant contribution for the residual fluorescence is a long-lived species (~30 ns) that possibly corresponds to the all-trans conformer with large donor-acceptor distance. In contrast to that, the n=2 compounds (Table 8, left column) showed diverse substituent-dependent fluorescence behavior. Especially the propargylic thioether **14a** did show high fluorescence quantum yield (0.47) and a mono-exponential decay with 24 ns lifetime and thus did not at all behave like an intramolecular donor-acceptor pair. In line with these results was the behavior of **14a** under singlet oxygen conditions (*vide supra*): no sulfoxide was formed even after prolonged reaction times and solely the oxidative cleavage of the propargyl group was observed.

Oxidation of other thioethers to the corresponding sulfoxides restores the strong fluorescence of undistorted DMPht but still with a moderate quenching by the sulfoxide group for several examples ($\mathbf{2}^{S=O}$, $\mathbf{3}^{S=O}$). Methionine derivatives (**10**–**12**) are in general less fluorescent than the corresponding cysteine derivatives (**13**–**14**), an unexpected behavior from the comparison of the model compounds **3** and **2**, respectively. The decay dynamics of the regioisomeric 3-/4-methylthiophthalimides **8** and **9** strongly differs (quantum yields for fluorescence 0.04 vs. 0.56) which can be explained by an additional decay channel only available for the geometrically more constrained compound **8**.

Experimental Section

Materials and Methods

All starting materials for substrate synthesis and solvents were commercially available. The detailed syntheses of the fluorescent 4,5-dimethoxyphthalimides are described in the SI. ^{1}H-NMR spectra were recorded on a Bruker Avance II 300 spectrometer operating at 300 MHz or on Bruker Avance III 500 spectrometer instrument operating at 500 MHz. Coupling patterns were designated as follows: s, singlet; d, doublet; dq, doublet of quartets; t, triplet; q, quartet; quin, quintet; m, multiplet. ^{13}C-NMR spectra were recorded either on a Bruker Avance II 300 spectrometer instrument operating at 75 MHz or on a Bruker Avance II 600 spectrometer instrument operating at 126 MHz. Melting points were measured on a MP50 Melting Point System by Mettler Toledo. IR spectra were obtained on a Si crystal Fourier-Transform spectrometer by Thermo Scientific (Nicolet 380 FT-IR). High-resolution mass (ESI) were obtained on a LC/MS Thermo Scientific LTQ Orbitrap XL instrument with FTMS analyzer. The elemental analyses were performed with an Elementar Vario EL.

Optical Spectroscopy

Absorption spectra were recorded on a Beckman Coulter UV-DU800. The samples were placed into quartz cells of 1 cm path length. All concentrations were 10^{-4} M. Emission and excitation spectra were carried out using a Perkin-Elmer LS-50B luminescence spectrometer. Samples were placed into quartz cells of 1 cm path length. For the determination of relative fluorescence quantum yields, quinine hemisulfate was used as reference with a standard solution in 0.1 M sulfuric acid. The probe and standard solutions were analyzed by UV-vis-absorption spectroscopy and the probe solution adopted in concentration to identical absorption at 370 nm, afterwards fluorescence spectra were determined and integrals were analyzed as described in the literature.[34] Time-resolved fluorescence measurements were performed with a *Horiba Science* DeltaFlexTM TCSPC-spectrometer equipped with a Delta DiodeTM DD-370 (excitation wavelength 370 nm). Data analyses were performed with *Horiba Science* Decay Analysis Software v6.8. All probes were investigated in quartz cuvettes (d=10 mm).

Computational Details

Structures were optimized in the ground state at the DFT level of theory using the 6–31+G(d,p) basis set and the CAM-B3LYP[35] and B3LYP functionals.[36–39] Also, the solvent (methanol) effect was considered by means of the polarizable continuum model (PCM).[40]

Then, vertical transitions were computed at the TD-DFT level of theory using the same functional and basis set. In addition, the Franck-Condon geometries were optimized in S_1 at the same level of theory to locate the emissive minima. From the minimum, a scan of the S–O distance coordinate was performed to explore the potential energy surface. All calculations were performed with the Gaussian 16 software package.[41]

Supporting Information

Syntheses of all fluorogenic compounds with spectroscopic data and time-resolved fluorescence decay curves; X-ray data of the phthalimides **3** and **14a**; computational details.

Acknowledgements

We thank the German Science Foundation DFG, the University of Cologne (starting grant) and the Spanish MINECO/FEDER (CTQ2017-87372-P) for support of this project.

Conflict of Interest

The authors declare no conflict of interest.

Keywords: electron transfer · fluorescence · phthalimides · quenching · thioethers

[1] J. R. Lakowicz, *Principles of Fluorescence Spectroscopy*, 3rd edition **2006**, Springer.
[2] M. A. El-Sayed, *J. Chem. Phys.* **1963**, *38*, 2834–2838.
[3] C. M. Marian, *WIREs Comput. Mol. Sci.* **2012**, *2*, 187–203.

[4] G. Dorman, H. Nakannura, A. Pulsipher, G. D. Prestwich, *Chem. Rev.* **2016**, *116*, 15284–15398.
[5] M. Chapran, R. Lytvyn, C. Begel, G. Wiosna-Salyga, J. Ulanski, M. Vasylieva, D. Volyniuk, P. Data, J. V. Grazulevicius, *Dyes Pigm.* **2019**, *162*, 872–882.
[6] J. D. Coyle, G. L. Newport, A. Harriman, *J. Chem. Soc. Perkin Trans. 2* **1978**, 133–137.
[7] J. D. Coyle, A. Harriman, G. L. Newport, *J. Chem. Soc. Perkin Trans. 2* **1979**, 799–802.
[8] A. Reiffers, C. T. Ziegenbein, L. Schubert, J. Diekmann, K. Thom, R. Kühnemuth, A. G. Griesbeck, O. Weingart, P. Gilch, *Phys. Chem. Chem. Phys.* **2019**, *21*, 4839–4853.
[9] H. Görner, A. G. Griesbeck, T. Heinrich, W. Kramer, M. Oelgemöller, *Chem. Eur. J.* **2001**, 7, 1530–1538.
[10] K.-D. Warzecha, H. Görner, A. G. Griesbeck, *J. Phys. Chem. A.* **2006**, *110*, 3356–3363.
[11] A. G. Griesbeck, J. Neudörfl, B. Goldfuss, S. Molitor, *ChemPhotoChem* **2017**, *1*, 355–362.
[12] P. Bencic, L. Mandic, I. Dzeba, I. T. Bujak, L. Biczok, B. Mihaljevic, K. Mlinaric-Majerski, I. Weber, M. Kralj, N. Basaric, *Sensors and Actuators B-Chem.* **2019**, *286*, 52–61.
[13] R. Orita, M. Franckevičius, A. Vyšniauskas, V. Gulbinas, H. Sugiyama, H. Uekusa, K. Kanosue, R. Ishige, S. Ando, *Phys. Chem. Chem. Phys.* **2018**, *20*, 16033–16044.
[14] T. Soujanya, R. W. Fessenden, A. Samanta, *J. Phys. Chem.* **1996**, *100*, 3507–3512.
[15] A. G. Griesbeck, S. Schieffer, *Photochem. Photobiol. Sci.* **2003**, *2*, 113–117.
[16] R. Perez-Ruiz, Y. Diaz, B. Goldfuss, D. Hertel, K. Meerholz, A. G. Griesbeck, *Org. Biomol. Chem.* **2009**, *7*, 3499–3504.
[17] S. Muhammad, C. G. Liu, L. Zhao, S. X. Wu, Z. M. Su, *Theor. Chem. Acc.* **2009**, *122*, 77–86.
[18] P. R. Sahoo, K. Prakash, P. Mishra, P. Agarwal, N. Gupta, S. Kumar, *Supramol. Chem.* **2017**, *29*, 417–429.
[19] A. G. Griesbeck, B. Öngel, M. Atar, *J. Phys. Org. Chem.* **2017**, *30*, e3741.
[20] Thiols: X. Liu, L. Gao, L. Yang, L. Zou, W. Chen, X. Song, *RSC Adv.* **2015**, *5*, 18177–18182.
[21] Cysteine: Y. Shen, X. Zhang, Y. Zhang, C. Zhang, J. Jin, H. Li, *Spectrochim. Acta Part A* **2017**, *185*, 371–375.
[22] A. G. Griesbeck, M. Oelgemöller, J. Lex, *J. Org. Chem.* **2000**, *65*, 9028–9032.
[23] A. G. Griesbeck, M. Oelgemöller, J. Lex, A. Haeuseler, M. Schmittel, *Eur. J. Org. Chem.* **2001**, 1831–1843.
[24] A. G. Griesbeck, N. Hoffmann, K.-D. Warzecha, *Acc. Chem. Res.* **2007**, *40*, 128–140.
[25] S. Farid, J. P. Dinnocenzo, P. B. Merkel, R. H. Young, D. Shukla, G. Guirado, *J. Am. Chem. Soc.* **2011**, *133*, 11580–11587.
[26] a) D. Rehm, A. Weller, *Ber. Bunsen-Ges. Phys. Chem.* **1969**, *73*, 834–839; b) D. Rehm, A. Weller, *Isr. J. Chem.* **1970**, *8*, 259–271.
[27] S. Fukuzumi, K. Shimoosako, T. Suenobu, Y. Watanabe, *J. Am. Chem. Soc.* **2003**, *125*, 9074–9082.
[28] K. Kishore, E. Anklam, A. Aced, K.-D. Asmus, *J. Phys. Chem. A* **2000**, *104*, 9646–9652.
[29] F. Hirayama, *J. Chem. Phys.* **1965**, *42*, 3163–3171.
[30] S. Speiser, *Chem. Rev.* **1996**, *96*, 1953–1976.
[31] R. Remy, C. G. Bochet, *Chem. Rev.* **2016**, *116*, 9816–9849.
[32] J. P. Dinnocenzo, A. M. Feinberg, S. Farid, *J. Phys. Chem. A* **2017**, *121*, 3662–2670.
[33] J. P. Dinnocenzo, A. Mark, S. Farid, *J. Org. Chem.* **2019**, *84*, 7840–7850.
[34] C. Würth, M. Grabolle, J. Pauli, M. Spieles, U. Resch-Genger, *Nat. Protoc.* **2013**, *8*, 1535–1550.
[35] T. Yanai, D. P. Tew, N. C. Handy, *Chem. Phys. Lett.* **2004**, *393*, 51–57.
[36] S. H. Vosko, L. Wilk, M. Nusair, *Can. J. Phys.* **1980**, *58*, 1200–1211.
[37] C. Lee, W. Yang, R. G. Parr, *Phys. Rev. B* **1988**, *37*, 785–789.
[38] A. D. Becke, *J. Chem. Phys.* **1993**, *98*, 5648–5652.
[39] P. J. Stephens, F. J. Devlin, C. F. Chabalowski, M. J. Frisch, *J. Phys. Chem.* **1994**, *98*, 11623–11627.
[40] J. Tomasi, B. Mennucci, R. Cammi, *Chem. Rev.* **2005**, *105*, 2999–3094.
[41] Gaussian 16, Revision A.03, M. J. Frisch, G. W. Trucks, H. B. Schlegel, G. E. Scuseria, M. A. Robb, J. R. Cheeseman, G. Scalmani, V. Barone, G. A. Petersson, H. Nakatsuji, X. Li, M. Caricato, A. V. Marenich, J. Bloino, B. G. Janesko, R. Gomperts, B. Mennucci, H. P. Hratchian, J. V. Ortiz, A. F. Izmaylov, J. L. Sonnenberg, D. Williams-Young, F. Ding, F. Lipparini, F. Egidi, J. Goings, B. Peng, A. Petrone, T. Henderson, D. Ranasinghe, V. G. Zakrzewski, J. Gao, N. Rega, G. Zheng, W. Liang, M. Hada, M. Ehara, K. Toyota, R. Fukuda, J. Hasegawa, M. Ishida, T. Nakajima, Y. Honda, O. Kitao, H. Nakai, T. Vreven, K. Throssell, J. A., Jr. Montgomery, J. E. Peralta, F. Ogliaro, M. J. Bearpark, J. J. Heyd, E. N. Brothers, K. N. Kudin, V. N. Staroverov, T. A. Keith, R. Kobayashi, J. Normand, K. Raghavachari, A. P. Rendell, J. C. Burant, S. S. Iyengar, J. Tomasi, M. Cossi, J. M. Millam, M. Klene, C. Adamo, R. Cammi, J. W. Ochterski, R. L. Martin, K. Morokuma, O. Farkas, J. B. Foresman, D. J. Fox, Gaussian, Inc., Wallingford CT, 2016. W. J. Hehre, R. Ditchfield, J. A. Pople, *J. Chem. Phys.* **1972**, *56*, 2257–2261.

Manuscript received: June 18, 2019
Revised manuscript received: August 7, 2019
Accepted manuscript online: August 9, 2019
Version of record online: September 11, 2019